VIRULENCE
2025, VOL. 16, NO. 1, 2450462
https://doi.org/10.1080/21505594.2025.2450462

Taylor & Francis
Taylor & Francis Group

RESEARCH ARTICLE

Characterization and genomic insights into bacteriophages Kpph1 and Kpph9 against hypervirulent carbapenem-resistant *Klebsiella pneumoniae*

Ye Huang [a,b], Yuan Huang[a,c], Zhiping Wu[d], Ziyue Fan[e], Fanglin Zheng[a,b], Yang Liu[b,f,g], and Xinping Xu [a,b]

[a]Jiangxi Institute of Respiratory Disease, Jiangxi Clinical Research Center for Respiratory Diseases, The Department of Respiratory and Critical Care Medicine, The First Affiliated Hospital, Jiangxi Medical College, Nanchang University, Nanchang, Jiangxi, P.R. China; [b]Jiangxi Hospital of China-Japan Friendship Hospital, Jiangxi, P.R. China; [c]Gerontology Department of The First Affiliated Hospital, Jiangxi Medical College, Nanchang University, Nanchang, Jiangxi, P.R. China; [d]Central Sterile Supply Department of The First Affiliated Hospital, Jiangxi Medical College, Nanchang University, Nanchang, Jiangxi, P.R. China; [e]Queen Mary College, Nanchang University, Nanchang, Jiangxi, P.R. China; [f]Department of Clinical Laboratory, Medical Center of Burn Plastic and Wound Repair, The First Affiliated Hospital, Jiangxi Medical College, Nanchang University, Nanchang, Jiangxi, P.R China; [g]Jiangxi Medical Center for Critical Public Health Events, The First Affiliated Hospital, Jiangxi Medical College, Nanchang University, Nanchang, Jiangxi, P.R. China

ABSTRACT

The increasing incidence of infections attributed to hypervirulent carbapenem-resistant *Klebsiella pneumoniae* (Hv-CRKp) is of considerable concern. Bacteriophages, also known as phages, are viruses that specifically infect bacteria; thus, phage-based therapies offer promising alternatives to antibiotic treatments targeting Hv-CRKp infections. In this study, two isolated bacteriophages, Kpph1 and Kpph9, were characterized for their specificity against the Hv-CRKp *K. pneumoniae* NUHL30457 strain that possesses a K2 capsule serotype. Both phages exhibit remarkable environmental tolerance, displaying stability over a range of pH values (4–11) and temperatures (up to 50°C). The phages demonstrate potent antibacterial and antibiofilm efficacy, as indicated by their capacity to inhibit biofilm formation and to disrupt established biofilms of Hv-CRKp. Through phylogenetic analysis, it has been revealed that Kpph1 belongs to the new species of *Webervirus* genus, and Kpph9 to the *Drulisvirus* genus. Comparative genomic analysis suggests that the tail fiber protein region exhibits the greatest diversity in the genomes of phages within the same genus, which implies distinct co-evolution histories between phages and their corresponding hosts. Interestingly, both phages have been found to contain two tail fiber proteins that may exhibit potential depolymerase activities. However, the exact role of depolymerase in the interaction between phages and their hosts warrants further investigation. In summary, our findings emphasize the therapeutic promise of phages Kpph1 and Kpph9, as well as their encoded proteins, in the context of research on phage therapy targeting hypervirulent carbapenem-resistant *Klebsiella pneumoniae*.

ARTICLE HISTORY
Received 23 April 2024
Revised 25 November 2024
Accepted 28 December 2024

KEYWORDS
Hypervirulent carbapenem-resistant strain; *Klebsiella pneumoniae*; phage characterization; genomic analysis; depolymerases

Introduction

Klebsiella pneumoniae, one of the "ESKAPE" pathogens, has the capacity to escape the killing ability of antibiotics through acquiring multiple resistant determinants and lead to the most widespread, severe infections with significant morbidity and mortality rates [1]. Carbapenem-resistant *Klebsiella pneumoniae* (CRKP), which harbor extended-spectrum β-lactamases (ESBLs) and/or carbapenemase, has been listed as one of the "Critical" priority pathogens by WHO due to a lack of effective antibiotics [2]. Recently, the emergence of hypervirulent Carbapenem-resistant *Klebsiella pneumoniae* (Hv-CRKp) represents a significant public health challenge as it is resistant to last-resort antibiotics and contains enhanced virulence factors, amplifying its threat level [3–5].

Various factors contribute to the virulence of *K. pneumoniae*, such as the capsule polysaccharide (CPS), lipopolysaccharide (LPS), aerobacterin, siderophore, fimbriae, and outer membrane protein [6,7]. CPS, the outermost layer on *K. pneumoniae*, serves as a protective barrier against antibiotics and host immune system [8]. CPS plays a pivotal role in the pathogenicity of *K. pneumoniae*, enabling it as a major virulence factor [8]. The *K. pneumoniae* CPS consists of repeating oligosaccharide units that form a polymer structure on the cell surface [9]. Differences in oligosaccharide combinations and residue modifications lead to the formation of distinct serotypes of capsules [10]. While over 79 capsular types of *K. pneumoniae* have been identified, the K2 type, along with K1, can trigger severe infections such as

CONTACT Xinping Xu xinpingxu@ncu.edu.cn
Supplemental data for this article can be accessed online at https://doi.org/10.1080/21505594.2025.2450462

typically pyogenic liver abscess, bacteremia, and meningitis, even in healthy individuals [11,12].

Phages are natural predators of bacteria. With the advantages of high specificity and low toxicity, phages, along with phage-derived enzymes, have been considered as a promising alternative to combat multidrug-resistant bacteria [13–15]. Many phages harbor specific polysaccharide depolymerases, which are mainly presented as phage structural proteins such as tail fibers, tail spikes, base plates, or tail tubular proteins [16]. These enzymes are crucial for recognizing and targeting the host cell and decomposing the CPS, extracellular polysaccharide (EPS), or/and LPS, components of the outer membrane in Gram-negative bacteria. This activity enables phage to reach the cell surface, bind to outer membrane receptors, and initiate infection [15]. CPS depolymerases showed specific selectivity to host with certain capsular serotypes. Therefore, both the phages themselves and phage-encoded depolymerases have the potential to act as anti-virulence agents for preventing and treating infections caused by Hv-CRKp [17]. Despite the promise of phages and depolymerases as treatments, there remains a notable gap in understanding and accessing phage agents that target the Hv-CRKp, especially strains with the K2 serotype [18–20].

This study aims to characterize two newly isolated lytic bacteriophages, Kpph1 and Kpph9, assess their efficacy against K2 type Hv-CRKp strain NUHL30457, and explore their genomic features for potential therapeutic application. Detailed characterization and comprehensive bioinformatic analysis of these bacteriophages were performed. Our findings will not only expand the phage library but also pave the way for developing innovative phage cocktail therapies tailored to address the specific challenge posed by Hv-CRKp.

Materials and methods

Bacterial strains and culture conditions

The clinical multidrug-resistant hypervirulent (CR-hvKP) *Klebsiella pneumoniae* strain NUHL30457 was previously isolated from a patient with severe burns [21]. The study and consent procedures were approved by the Ethical Committee of the First Affiliated Hospital of Nanchang University (FAHNU) in compliance with the Declaration of Helsinki principles (CDYFY-IACUC-202403QR003). Verbal consent was obtained from the participant before the strain isolation. Strain NUHL30457 has been categorized as capsular serotype K2 and sequence type (ST) 86, and is capable of producing both KPC-2 and NDM-1 type carbapenemases. This strain was utilized as the host bacterium for phage isolation and characterization, and it was routinely cultured in Luria – Bertani (LB) medium (10 g/L tryptone, 5 g/L yeast extract, 5 g/L NaCl) at 37°C.

Phages isolation and purification

Phages were isolated from sewage water collected from a local wastewater treatment facility in Nanchang, Jiangxi. The isolation, purification, and characterization of phages were carried out as previously described, with the modest modification [22]. Briefly, the untreated sewage samples were centrifuged at 8,000 × g for 30 min at 4°C, then the supernatant was filtered through a 0.22 μm membrane syringe filter to remove bacterial cells. Following this, the double agar overlay plaque assay was performed by mixing 100 μL of filtered sewage samples, 100 μL of bacterial host culture at OD_{600} 0.3, and 4 mL of molten soft agar (0.7% w/v agar), which was then poured over solidified 1.5% LB agar plate. After overnight incubation at 37°C, clear plaques could be observed. Single phage plaque was picked using sterile micropipette tips and re-suspended in 1 mL SM buffer (2 g/L $MgSO_4.7\,h_2O$, 5.8 g/L NaCl, 50 mL/L 1 M Tris-HCl (pH7.5), 0.01% Gelatin (m/v)), and then purified using a 0.22 μm membrane syringe filter. Phage plaques were isolated and further purified through three rounds of double agar overlay plaque assay until uniform plaques were formed.

Generation of high-titer phage stocks

Purified phages were amplified by mixing 500 μL of phage suspension and 50 mL of bacterial host culture at OD_{600} 0.3. The mixture was then incubated 2 h at 37°C with 180 rpm as previously described [23]. After centrifugation and filtration, the phage suspension was treated with DNase I and RNase A (10 μg/mL final) for 2 h at 37°C, followed by precipitation with the addition of NaCl (1 M final concentration) and polyethylene glycol (PEG) 8000 (10% w/v) and incubated at 4°C overnight. Following centrifugation at 10,000 × g at 4°C for 20 min, the precipitated phage lysates were resuspended in 1 mL SM buffer. The high-titer phage suspension was stored at 4°C for further analysis.

Transmission electron microscopy

Phage morphology was examined using transmission electron microscopy (TEM) as previously described [24]. A high-titer phage preparation (titer >10^9 PFU/mL) of purified phages was applied to 200-mesh carbon-coated copper grids for 1 min and negatively

stained with 2% uranyl acetate, followed by the removal of excess stain. The grids were then viewed under a transmission electron microscope (JEM1400, JEOL, Japan) at 80 kV.

Host range determination

The host ranges of the phages were assessed using spot tests against 15 clinical isolates of *Klebsiella pneumoniae* collected from the FAHNU in China. The Ethical Committee of the FAHNU approved the use of strains for this study and verbal consents were also obtained (CDYFY-IACUC-202403QR003). Approximately 10^6 PFU of phage in 10 µL of LB broth were spotted onto a bacterial lawn and incubated overnight. Phage-sensitive strains produced clear, transparent plaques on the agar.

Optimal multiplicity of infection of phages

The optimal multiplicity of infection (MOI) was determined as previously described with some modifications [25]. The host strain was incubated with diluted phage stock (10^1-10^9 PFUs/mL) at MOIs ranging from 0.000001 to 100. The mixtures were incubated at 37°C with shaking at 180 rpm for 3.5 hours. Phage titers were assessed using the double agar overlay method. The MOI resulting in the highest phage titer was identified as the optimal MOI.

One-step growth curve assays

One-step growth curve and burst size of phage were determined as described previously, with modifications [26,27]. Briefly, host bacterium was incubated at 37°C until reaching an OD_{600} of 0.3. Subsequently, a mixture of 9.9 mL host solution and 100 µL of the phage suspension were prepared to achieve a multiplication of infection (MOI) of 0.01. The mixture was incubated at 37°C for 5 min and then centrifuged at 12,000 × g for 2 min. The resulting pellet was washed and then suspended in LB medium. A 1/100 dilution was made by transferring 100 µL bacteria-phage mixture to 9.9 mL fresh prewarmed LB medium in flask A. This was followed by a 1/10 dilution by transferring 1 mL of solution from flask A to flask B, which contained 9 mL of prewarmed LB medium. Samples of 100 µL were periodically taken from flask A or B at 2-min intervals, mixed with 100 µL host incubation at OD_{600} 0.3 in 4 mL of semi-solid agar and overlayed on LB plates. The plates were then incubated overnight at 37°C, and the plaque-forming units (PFUs) were counted. The experiment was conducted in triplicate.

Host killing curve assays

The bacterial killing ability was assessed by exposing Kp strain 30,457 (about 10^8 CFU/mL) to phage at MOIs (100, 10, 1, 0.1, 0.01, 0.001, 0.0001, 0.00001, and 0.000001). The optical density at 600 nm was measured using Bioscreen C, and data were collected at 20 min intervals for 24 h. The bacterial incubation without mixing the phage solution was used as a negative control, while sterile LB medium was set as blank control. The experiment was conducted in triplicate.

Thermal and pH stability

The temperature stability of the phages was assessed by combing 100 µL phage suspensions (~10^8 PFU/mL) with 900 µL SM buffer and incubating at 4, 25, 37, 50, 60, and 70°C for 1 to 3 hours. After incubation, 100 µL aliquots of the phage solutions were collected for analysis at 1-hour intervals [28]. To evaluate the pH stability, 100 µL of phage suspensions were incubated with SM buffer at pH levels ranging from 1 to 14 for 1 to 3 hours, and phage viability was determined [29]. Phage titer was measured using serial dilutions and the double agar overlay plaque assay technique.

Biofilm inhibition and disruption assay

Biofilm formation and treatment were performed as previously described with minor modifications [29,30]. Briefly, overnight bacterial cultures were diluted in fresh TSB medium to a concentration of 10^6 CFU/mL. Then, 125 µL of the diluted culture was added into a 96-well sterile polystyrene microtiter plate. For the biofilm inhibition assay, host cultures were immediately exposed to phage infection varying MOI (ranging from 0.001 to 10) and then incubated at 37°C without rotation for 48 h. Negative control wells containing untreated culture and blank control containing sterile LB medium were included in the experiment. To measure the biomass of biofilms, the planktonic cells and media were removed, and the adhered biofilms were washed three times with PBS buffer and then air dried. Subsequently, the biofilms were stained with 150 µL 0.1% (w/v) crystal violet for 15 min, washed three times with ddH_2O until the wells of blank control were colorless. Finally, the dye was solubilized in 150 µL 95% (v/v) absolute ethanol and the absorbance at 590 nm was measured using a microplate reader. For biofilm disruption assay, all bacterial cultures were incubated without phage infection for 48 h to form mature biofilm. Following the incubation period, the bacterial culture was exposed to phage preparations of

varying titers and then further incubated at 37°C for 24 hours. Subsequent biofilm measurements were conducted following the same protocol as previously described. Data are presented as means ± standard deviations (SD) and were analyzed using one-way ANOVA tests with GraphPad Prism 8.4.3. Differences were considered statistically significant at p values of < 0.05 (*), < 0.01 (**), or < 0.001 (***).

Phages DNA extraction and whole genome sequencing

Phage DNA was extracted from phage stock (>10^9 PFU/mL) using the phenol-chloroform-isoamyl alcohol method as described previously [31]. Briefly, DNase I and RNase A (final concentration of 1 μg/mL each) were added and the mixture was incubated at 37°C for 1 hour. 0.5 mol/L EDTA and 10 mg/mL proteinase K were then added to the lysate to final concentrations of 20 mmol/L and 50 μg/mL, respectively. The solution was thoroughly mixed and then incubated in the water -bath at 56°C for 1 h. Subsequently, 1/10 volume of Tris-HCl (1 M, pH 8.0) and equal volume of Tris-phenol was added to facilitate DNA extraction. After centrifuging at 10,000 × g for 10 min, the upper aqueous phase containing the phage was collected, followed by the addition of an equal volume of phenol-chloroform-isoamyl alcohol (25:24:1) and repeated centrifugation. The upper aqueous phase was then subjected to two rounds of chloroform extraction, followed by the addition of double the volume of isopropanol to precipitate the DNA at −20°C for 1 h. Upon subsequent centrifugation at 10,000 × g for 10 min, the supernatant was carefully removed, and 1 mL of 70% ethanol was added to resuspend the DNA. After centrifugation and air drying, the phage DNA was redissolved in 50 μL of ddH_2O. DNA concentration was measured using a Nanodrop 2000, and the purified phage DNA was sent to Meige Biotech Co. for whole-genome sequencing. The sequencing library was prepared using the Illumina Nextera DNA Flex Library Prep Kit and sequenced using the Illumina NovaSeq.

Bioinformatic analysis

Raw reads were quality-controlled by trimming primers and filtering out low-quality reads with Soapnuke [32]. BWA was performed to remove the host genome contamination [33]. The high-quality sequences were assembled using Megahit [34] and contigs were assigned to known phage sequences using CheckV [35]. The quality-controlled reads from each phage were mapped to the assembled contigs. Resulting sam files were transformed into bam files and sorted, and coverage information of contigs was computed with Samtools [36]. Life cycles of phages were predicted by PhageAI [37]. Protein-coding genes were identified from phage genome and gene functions were annotated using RAST [38] and Phanotate [39], and verified using Blastp. tRNA Scan-SE was used to scan the possible tRNA genes of phage genomes [40]. Potential virulence and drug resistance genes were identified by searching through VFDB [41] and ResFinder [42]. Phage genome annotation and visualization was carried out using Proksee [43]. The annotations of structural proteins in phages were verified using PHANNS [44]. HHpred and Swiss-model were utilized for protein homology detection and structure prediction [45,46]. The taxonomy classification was determined by retrieving and downloading reference phage genomes using BLASTN, followed by the identification of conserved proteins using Roary [47]. The concatenated sequences were aligned using mafft [48] with 85% similarity. Phylogenetic trees were then constructed based on the neighbor-joining method using Mega7 [49]. The pairwise intergenomic distances/similarities of phage genomes were computed using VIRIDIC [50]. The assignment of viruses to genera (≥70% similarity) and species (≥95% similarity) follows the International Committee on Taxonomy of Viruses (ICTV) genome identity thresholds [50]. Genomic comparative analysis of phages was preformed using Viptree based on phage genome-wide sequence similarities [51].

Results

Morphology of phage Kpph1 and Kpph9

Klebsiella phages Kpph1 and Kpph9 were isolated from wastewater samples obtained near a hospital in Nanchang, China. The host was the carbapenem-resistant hypervirulent *Klebsiella pneumoniae* strain NUHL30457. Both phages exhibit specific lytic activity against NUHL30457. Kpph1 and Kpph9 could produce clear plaques of 5–7 mm and 3–5 mm in diameter, respectively, surrounded by diffusing translucent halos on the bacterial lawn (Figure 1a,b). The halo region surrounding each plaque indicates phage-encoded depolymerase activity. TEM analysis of the purified phages revealed distinctive morphologies. Kpph1 displayed an icosahedral head measuring 60 nm in diameter, accompanied by a about 200 nm long flexible non-contractile tail. On the other hand, Kpph9 featured a 10 nm neck appendage and a short tail measuring 40 nm in length (Figure 1c,d).

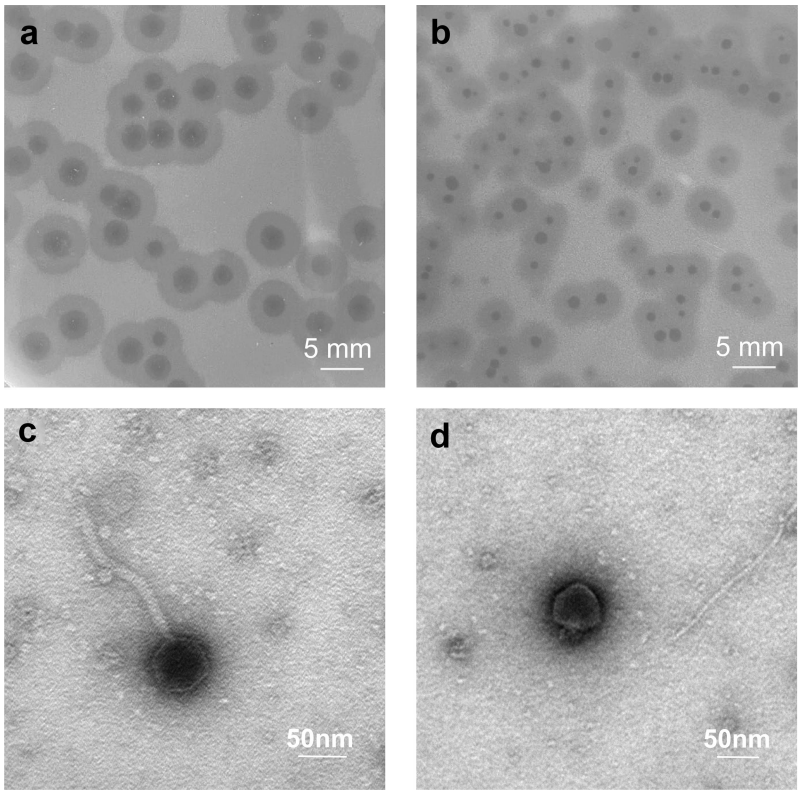

Figure 1. Morphology of phage Kpph1 and Kpph9. (a and b) Phage plaques of Kpph1 (a) and Kpph9 (b) on the plate, and TEM observation of Kpph1 (c) and Kpph9 (d).

Host range of phages

Phages Kpph1 and Kpph9 demonstrated a narrow lytic activity range against 15 *Klebsiella pneumoniae* strains tested. Both phages specifically lysed only K2-type strains among those with different capsular types (K1, K2, and K64) (Supplementary Fig. S1). Regarding sequence types (ST), Kpph1 targets exclusively ST65, while Kpph9 can lyse both ST65 and ST25.

Characterization of the phage infection

The optimal multiplicities of infection (MOI) and one-step growth curves were determined to assess phage growth parameters. Both phages exhibited an optimal MOI of 0.000001 (Figure 2a,b). Kpph1 had a 16-minute latent period, a 13-minute lytic cycle duration, and an average burst size of 400 PFU/cell (Figure 2c). In contrast, Kpph9 exhibited a 11-minute latent period, a 15-minute lytic cycle duration, and an average burst size of 25 PFU/cell (Figure 2d).

Phage temperature and pH stability

To assess the environmental adaptability and stability, experiments were conducted on phages Kpph1 and Kpph9 across wide pH levels (1 to 13) (Figure 2e,f) and temperature ranges (4°C to 70°C) (Figure 2g,h). Both phages exhibited tolerance to a broad pH range (pH 4–11) and resistance to high temperatures (up to 50°C), with only slight reductions in titer after 3 hours of incubation. Sharp decreases in phage viability were observed after being treated at extreme temperatures (>60°C) or under highly acidic or alkaline conditions (pH < 3 or pH > 11).

Host killing curve of phages

To characterize the abilities of phages against their Hv-CRKp host, the host killing curves were generated for both phages. The host killing curve of Kpph1 was derived at MOIs ranging from 0.0001 to 1000. The most significant inhibition of bacterial growth, as indicated by no increase in OD600 nm, was observed at MOI 1000, MOI 100, and MOI 10 for the initial 7 h, 3 h, and 2 h of infection, respectively (Figure 3a). Effective growth suppression was observed for the first 4 hours at MOI 1, MOI 0.1, and MOI 0.01, but by 7 h post-infection resistance began to emerge under all conditions (Figure 3a). For Kpph9, the host killing curve was established across MOIs from 0.00001 to 10.

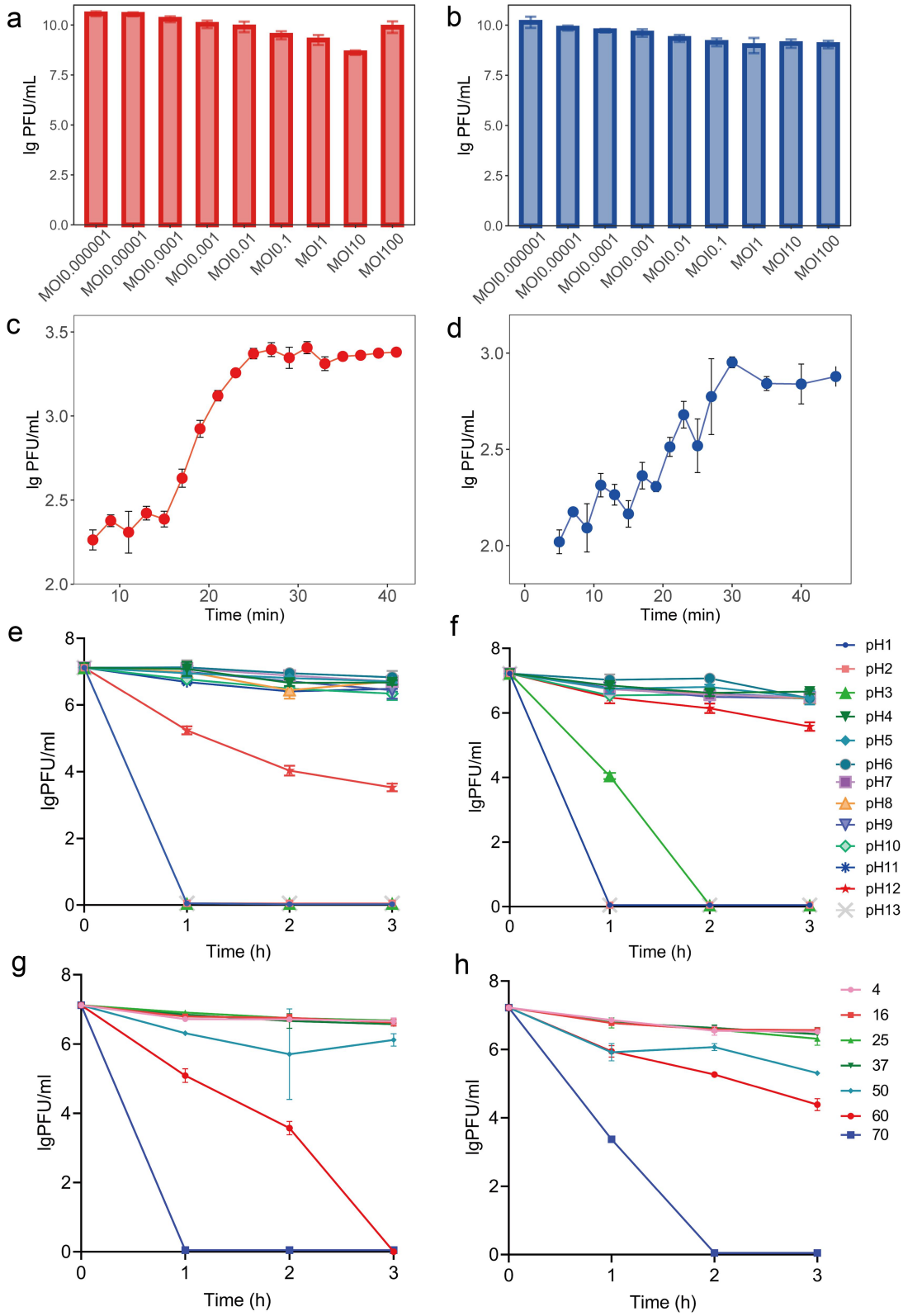

Figure 2. Characterization of the phage infection. (a and b) optimal MOIs ($n = 5$) of Kpph1 (a) and Kpph9 ($n = 5$) (b). (c and d), one-step growth curves of Kpph1 ($n = 5$) (c) and Kpph9 ($n = 5$) (d). (e and f) stabilities of Kpph1 ($n = 5$) (e) and Kpph9 ($n = 5$) (f) under pH 1 to 13. (g and h) stabilities of Kpph1 ($n = 5$) (g) and Kpph9 ($n = 5$) (h) under temperature 4°C to 70°C.

The greatest suppression of host growth was noted at MOI 10 and MOI 1 during the initial 7 h and 5 h, respectively, without increases in OD600 nm (Figure 3b). Similar to Kpph1, the resistance to Kpph9 manifested at 7 h post-infection (Figure 3b).

Inhibition and disruption of biofilm by phages application

To characterize the inhibition capacity of phages on host biofilm formation, solutions of phages Kpph1 and Kpph9 at different MOIs were applied before the biofilm formation process. The results demonstrated the substantial disruption caused by both Kpph1 and Kpph9 on the biofilm formation of *K. pneumoniae* NUHL30457 with MOIs ranging from 0.01 to 10, as determined by the reductions in OD590 values of 19.7% to 55.4% for Kpph1 and 24.1% to 55.6% for Kpph9 (Figure 3c). The maximum antibiofilm activity was observed at an MOI of 1 for both phages ($p < 0.0001$). To assess the phages' potential in degrading mature biofilms, biofilms aged 48 hours were exposed to phages at various MOIs. It was found that biofilms were significantly disrupted after a 24-hour treatment with Kpph1 and Kpph9 at all tested MOIs, except for Kpph9 at an MOI of 1 ($p = 0.069$) (Figure 3d).

Phylogenic analysis

Comparison with the genomes deposited in NCBI databases revealed that Kpph1 was most closely related to the *Klebsiella* phage LF20 (with a query coverage of 94% and an overall nucleotide identity of 96.68% as determined by BLASTn), a member of the Drexlerviridae family, *Webervirus* genus. On the other hand, Kpph9 was closely related to *Klebsiella* phage QL (with a query coverage of 95% and an overall nucleotide identity of 98.87%), which is affiliated with the Autographiviridae family, *Drulisvirus* genus. To illustrate the evolutionary relationship between the phages under study and reference *Klebsiella* phages, multiple alignments were performed based on protein sequences present in all phages from the same genus were performed (Table S1). Phylogenetic trees constructed

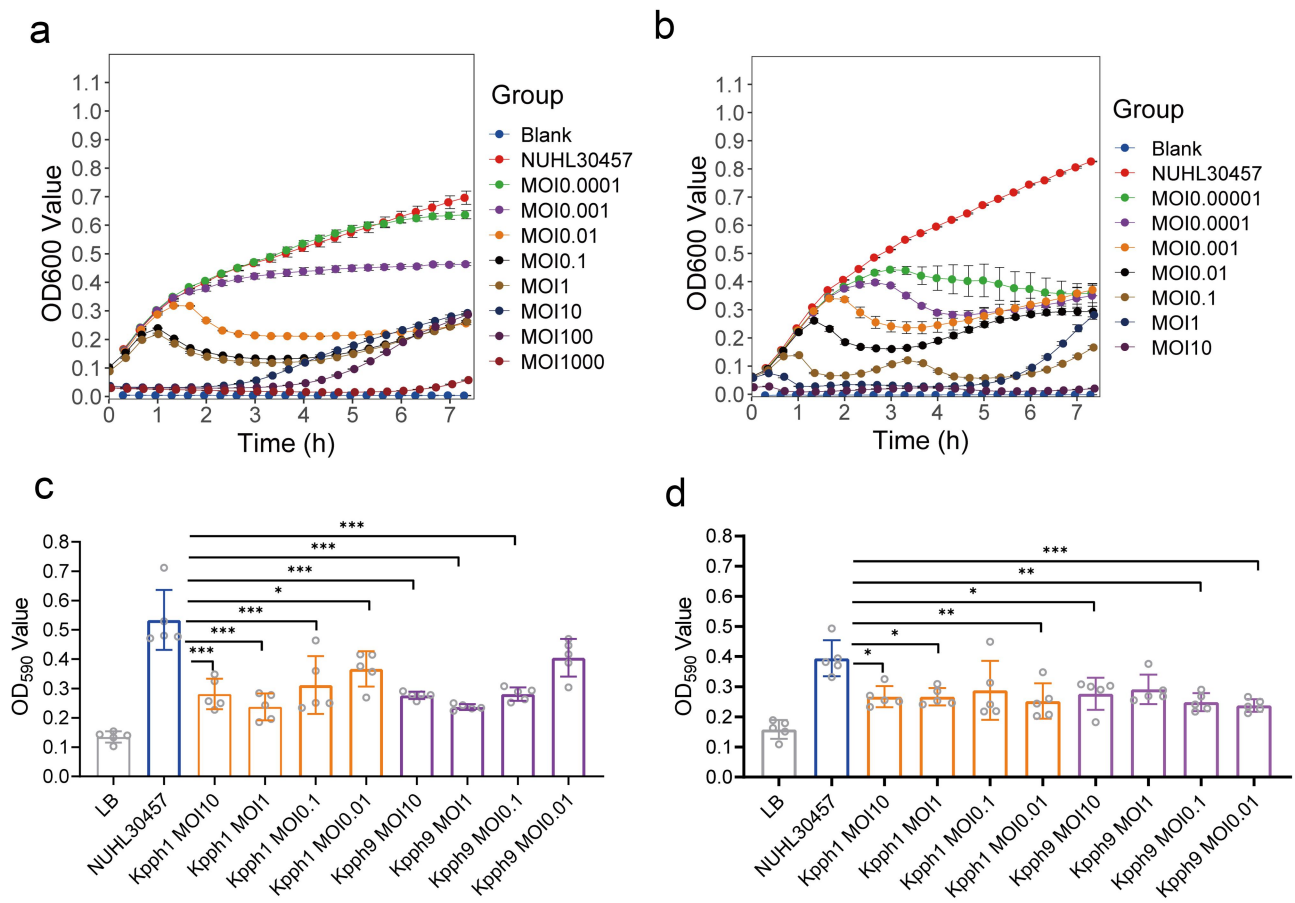

Figure 3. Antibacterial and antibiofilm abilities of Kpph1 and Kpph9. (a and b) Host killing curves of Kpph1 ($n = 5$) (a) and Kpph9 (b) ($n = 5$) at different MOIs. (c) The inhibition capacity of phages on host biofilm formation ($n = 5$). (d) The effect of phages in degrading mature biofilms ($n = 5$). Values are expressed as means ± the SD. *$p < 0.05$; **$p < 0.01$, ***$p < 0.001$ (one-way ANOVA).

based on 12 core proteins and placed Kpph1 and phage LF20 in a distinct cluster with phage KOX1, vB KpnS IMGroot, vB KpnS Call, vB KpnS Domnhall, vB KpnS Alina, and vB KpnS KpV522, diverging from the Kp36 virus cluster that includes phage Kp36, GH-K3, and KLPN1, among others (Supplementary Fig. S2). Through pairwise intergenomic similarities among phage genomes, it revealed that Kpph1 displayed the highest similarity of 93.98% with *Klebsiella* phage LF20, followed by pairwise similarities ranging from 83.65% to 86.10% with members of the KOX1 cluster (Table S2 and Supplementary Fig. S3). Phage Kp36 was taken as the reference species for the genus *Webervirus*. Kpph1 exhibited a nucleotide similarity of 75.92% with Kp36, suggesting that it represents a new species within the genus *Webervirus*.

Kpph9 shared 22 core proteins with the reference genomes of the genus *Drulisvirus* (Table S3). Phylogenetic analysis of concatenated core proteins demonstrated that Kpph9 was closely related to phage QL and KpV74, with intergenomic similarities being 93.68% and 86.92%, respectively (Table S4 and Supplementary Fig. S4-S5). Therefore, it is proposed that Kpph9 be classified as a new species within the genus *Drulisvirus*.

Genomic analysis of phages

To ascertain the genomic characteristics of the phages and validate their suitability for phage therapy applications, the genomes of Kpph1 and Kpph9 were sequenced and analyzed. The phage Kpph1 possesses a circular double-stranded DNA genome with a size of 50,883 bp and a GC content of 50.68%. It encodes 80 open reading frames (ORFs), 56 of which are situated on the plus strand, and 24 on the minus strand as identified by RAST (Figure 4a). On the other hand, phage Kpph9 comprises linear double-stranded DNA genome measuring 43,645 bp in length with a 54.01% GC content, harboring 56 ORFs, all situated on the plus strand (Figure 4b). Analysis revealed that 41 of the ORFs in Kpph1 (51.3%) and 26 in Kpph9 (46.4%) are involved in encoding functional proteins. Additionally, both genomes containing ORFs encoding hypothetical proteins, with 39 out of 80 ORFs (48.7%) in Kpph1 and 30 out of 56 ORFs (53.6%) in Kpph9. The initiation codons for Kpph1 are represented by 93.8% ATG, 4.9% GTG, and 1.3% GAC. Regarding stop codons, TAA is utilized in 58.0% of cases, followed by TGA (24.7%) and TAG (17.3%) in Kpph1. In contrast, the initiation codons for Kpph9 are mainly ATG (89.2%), with TTG and GTG accounting for 5.4% each. The stop codons in Kpph9 are distributed as 53.5% for TAA, 32.1% for TGA, and 14.4% for TAG.

Functional annotation

The annotated genes of Kpph1 and Kpph9 can be primarily classified into six functional groups: phage morphogenesis and packaging (e.g. the major capsid protein, portal protein, head maturation protease, and capsid assembly scaffolding protein); tail structure (including the tail tape measure protein, major tail protein, minor tail protein, tail tubular protein, tail fiber protein, and the phage collar); DNA replication/modification (e.g. DNA primase, DNA repair exonuclease, DNA endonuclease, DNA helicase, DNA polymerase, single-stranded DNA binding protein, and deoxynucleoside monophosphate kinase (dNMP kinase)); transcription (DNA-directed RNA polymerase, polyribonucleotide nucleotidyltransferase, and transcriptional regulator); host lysis proteins (endolysin, holin, spanin, and internal virion lysozyme motif); and other functions (e.g. Eaa protein, membrane protein, acid phosphatase, metallo-phosphoesterase, peptidase, and DNA adenine methyltransferase) (Figure 4a,b). To evade host defenses, Kpph1 encodes a DNA adenine methyltransferase (ORF29) (DAM), a DNA methylase (ORF44), and a cytosine DNA methyltransferase (ORF45), which are believed to protect phage DNA from host restriction endonucleases (Figure 4a). The absence of tRNA genes in the genomes of Kpph1 and Kpph9 indicates that these phages rely entirely on the host cells for protein synthesis. Moreover, the lack of integrase genes confirms that Kpph1 and Kpph9 are virulent phages, consistent with the PhageAI predictions regarding their life cycle. Furthermore, the absence of genes associated with virulence, pathogenicity, or drug resistance suggests their promising potential as therapeutic agents.

Host lysis strategy of phages and putative depolymerase identification

The genes associated with host lysis in the genomes of phages Kpph1 and Kpph9 include endolysins (ORF37 for Kpph1 and ORF55 for Kpph9), holins (ORF36 for Kpph1 and ORF54 for Kpph9), and spanins (ORF38 for Kpph1, and ORF 35 and ORF 53 for Kpph9). These genes potentially hydrolyze peptidoglycan, contribute to the disruption of the host cell membrane, and facilitate the liberation of progeny phage particles. ORF19 and ORF20 in the Kpph1 genome, and ORF48 and ORF56 in the Kpph9 genome, are characterized as (central) tail fiber/spike proteins that are hypothesized to encode depolymerases – enzymes that break down the host cell's capsular polysaccharide, aiding the phage in attaching to receptors on the cell's outer membrane (Figure 5a).

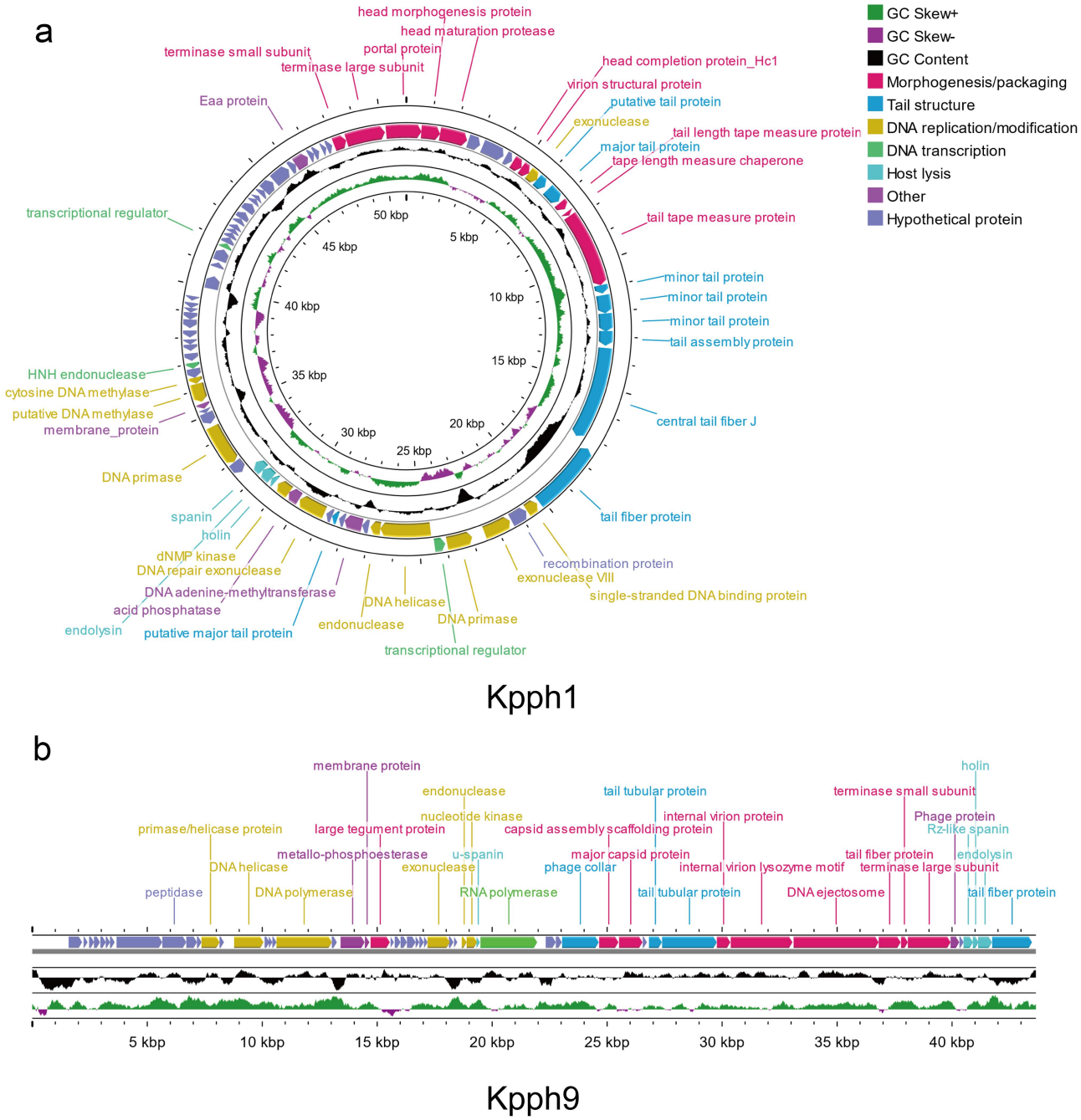

Figure 4. Genomic information for phages Kpph1 and Kpph9. (a and b) genomic maps of Kpph1 (a) and Kpph9 (b). Phage protein-coding genes were identified and annotated using RAST and Phanotate, and verified using Blastp. Genome visualization was carried out using proksee.

Among the tail fiber/spike proteins encoded by Kpph1 and Kpph9, only ORF20 of Kpph1 exhibited a high sequence identity and structural similarity of 97.79% to a known depolymerase (PDB: 7LZJ_A), as predicted by HHpred and Swiss-model (Figure 5a–c). ORF19 from Kpph1 is predicted to be a central tail fiber protein. For ORF19 from Kpph1, the amino acid sequence 718–821 displayed a 96.97% match with pectate lyase (PDB: 3B4N_A) (Figure 5a,b). ORF56 from Kpph9 is predicted to encode a tail spike protein; its amino acid sequence 10–300 shows similarity to pectate lyase (PDB: 7CHU_A), and sequence 400–576 corresponds precisely with endoglucanase (PDB: 8AG9_A), exhibiting a 100% probability (Figure 5a–e). Additionally, ORF48 from Kpph9, annotated as a short non-contractile tail fiber protein, demonstrates a 99.8% match with model 7Y22_f (Figure 5a–d). The amino acid sequence 1–103 of ORF48 is likely involved in lipopolysaccharide degradation, indicated by a 91.31% similarity to 6W4Q_A (Figure 5a).

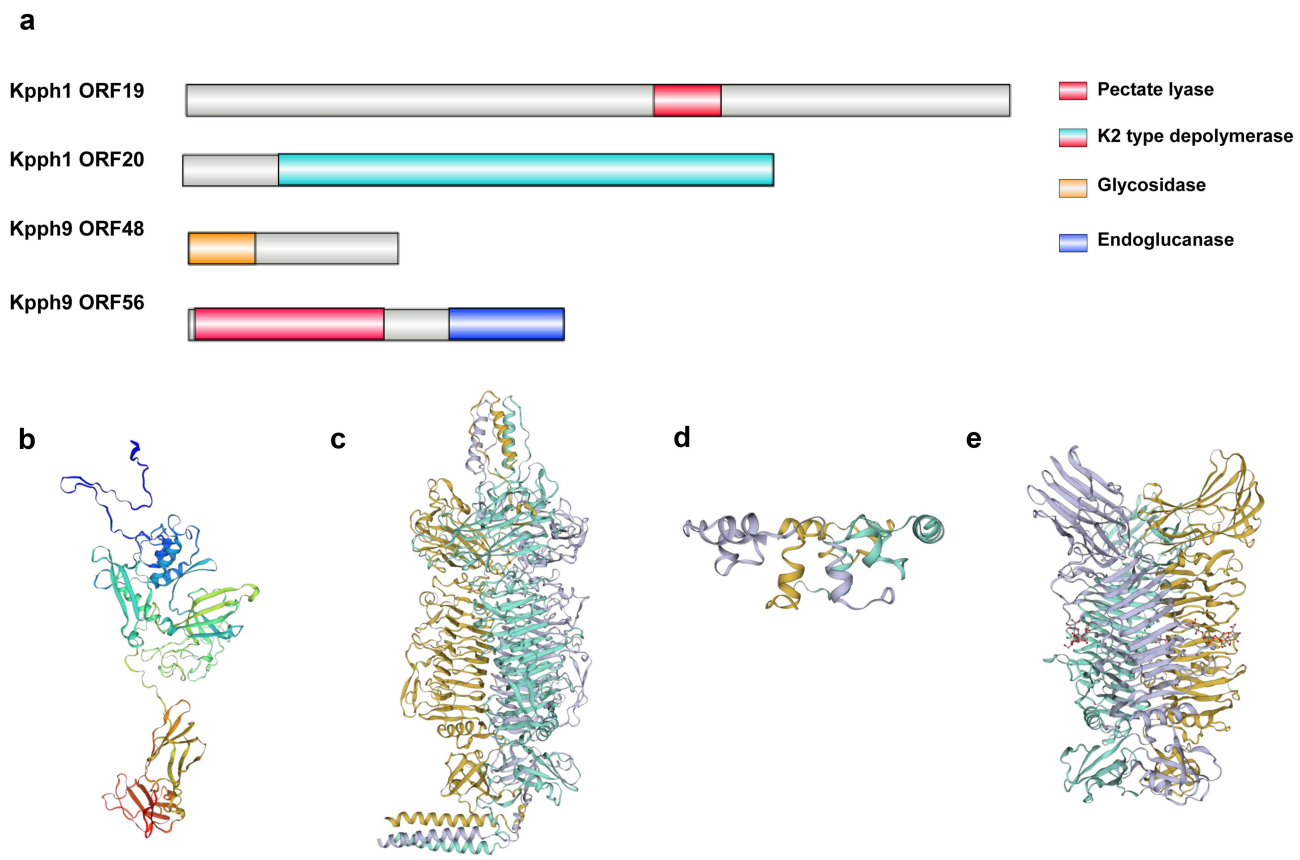

Figure 5. Protein structural prediction of depolymerases of Kpph1 and Kpph9. (a) Protein domains predicted by HHpred. (b and c) three-dimensional structure of Kpph1 ORF19 (b) and ORF20 (c) predicted by Swiss-Model. (d and e) three-dimensional structure of Kpph9 ORF48 (d) and ORF56 (e) predicted by Swiss-Model.

Comparative genomic analysis of phages

To demonstrate the genomic discrepancy of Kpph1 and Kpph9 with reference phages, genomic alignments were conducted for the phages (Figure 6 and 7).

Among the studied genomes of the *Webervirus* genus, only three proteins – the terminase large subunit, the central tail fiber protein, and DNA helicase – are markedly conserved, exhibiting similarities exceeding 94%. The analysis revealed that the genetic sequences encoding proteins involved in DNA metabolism and morphogenesis-related functions shared a nucleotide identity over 90% between Kpph1 and LF20, except for the sequence 8700–12439 (annotated as the tail length tape measure protein), 20938–22782 (encoding a recombination protein and exonuclease), and the region 42,084–48937 within Kpph1 (Figure 6). The latter region encodes multiple hypothetical proteins and demonstrates notable diversity among the aligned genomes. Within this sequence, a protein functioning as a transcriptional regulator has been identified. The genes locate in this specified region exhibit a striking similarity of 99% to sequences from *K. pneumoniae* sequences.

Klebsiella phages within the *Drulisvirus* genus are primarily clustered into three groups principally based on their host specificity. Phage Kpph9 is grouped with phages QL and KpV74; all of which target the K2 serotype of *K. pneumoniae*. The prototypical species for the *Drulisvirus* genus, phage Kp34 (which targets the K63 serotype), is clustered together with phiBO1E and vB_Kp2, whereas phages KpV475 and KpV71 specifically target the K1 capsular type. Genomic analysis of the *Drulisvirus* genus has revealed a set of highly conserved proteins with similarities exceeding 96% including DNA helicase, the head-tail adaptor protein, the head scaffolding protein, and the terminase large subunit. However, there is significant variability observed in the tail fiber proteins encoded by phages within this genus. As compared to phage QL, Kpph9 lacks two HNH endonucleases within the regions 13,-963–14424 and 17,710–18177, but has acquired an endonuclease spanning 18,678–18890, a spanin in the region 19,335–19451, a membrane-associated initiation of head vertex in 10,107–10316, and a 1hypothetical protein encompassed by 16,666–16830 (Figure 7).

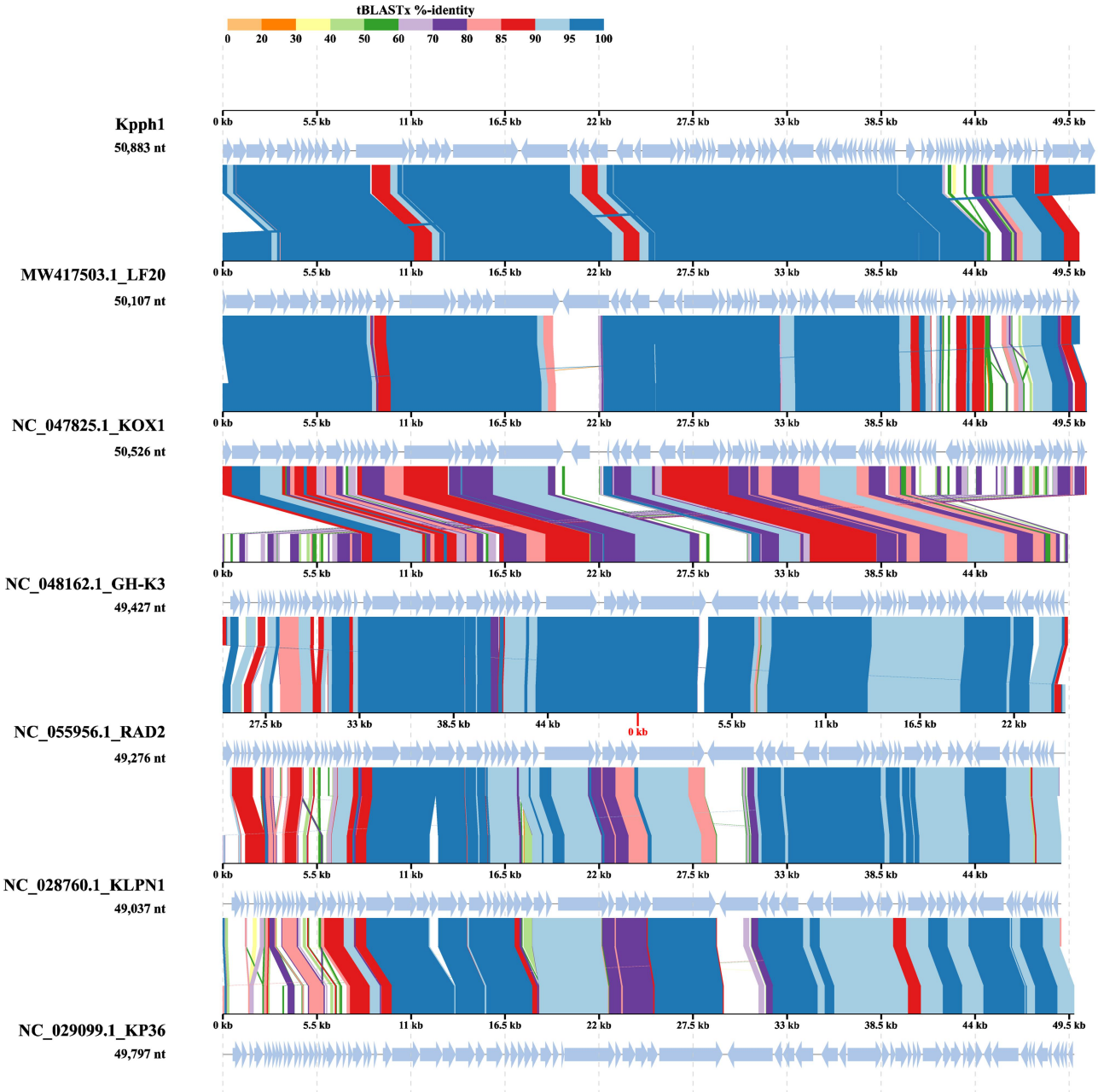

Figure 6. Genomic comparative analysis of Kpph1 and the mostly related phages in *Webervirus* genus was preformed using viptree based on genome-wide sequence similarities.

Discussion

Klebsiella pneumoniae is recognized as one of ESKAPE pathogens, a group posing a significant and urgent threat to global public health. As multidrug-resistant bacterial infections, whether in planktonic or biofilm form, continue to challenge traditional treatment methods, phages are increasingly being explored as an alternative therapy. However, phage therapy remains considered an experimental strategy, underscoring the need for comprehensive characterization of specific phages intended for this therapeutic purpose before clinical trials can commence [52].

The current study, explored the physiological, biochemical, and genomic characteristics of the phages Kpph1 and Kpph9. Phylogenetic trees based on nucleotide and protein sequences demonstrated that Kpph1 was affiliated with *Drexlerviridae*, and Kpph9 was a member of *Autographiviridae*. Both phages exhibited specific lytic activity against K2 capsular type *K. pneumoniae* and formed clear plaques on overlay plates. When co-cultivated with Hv-CRKp

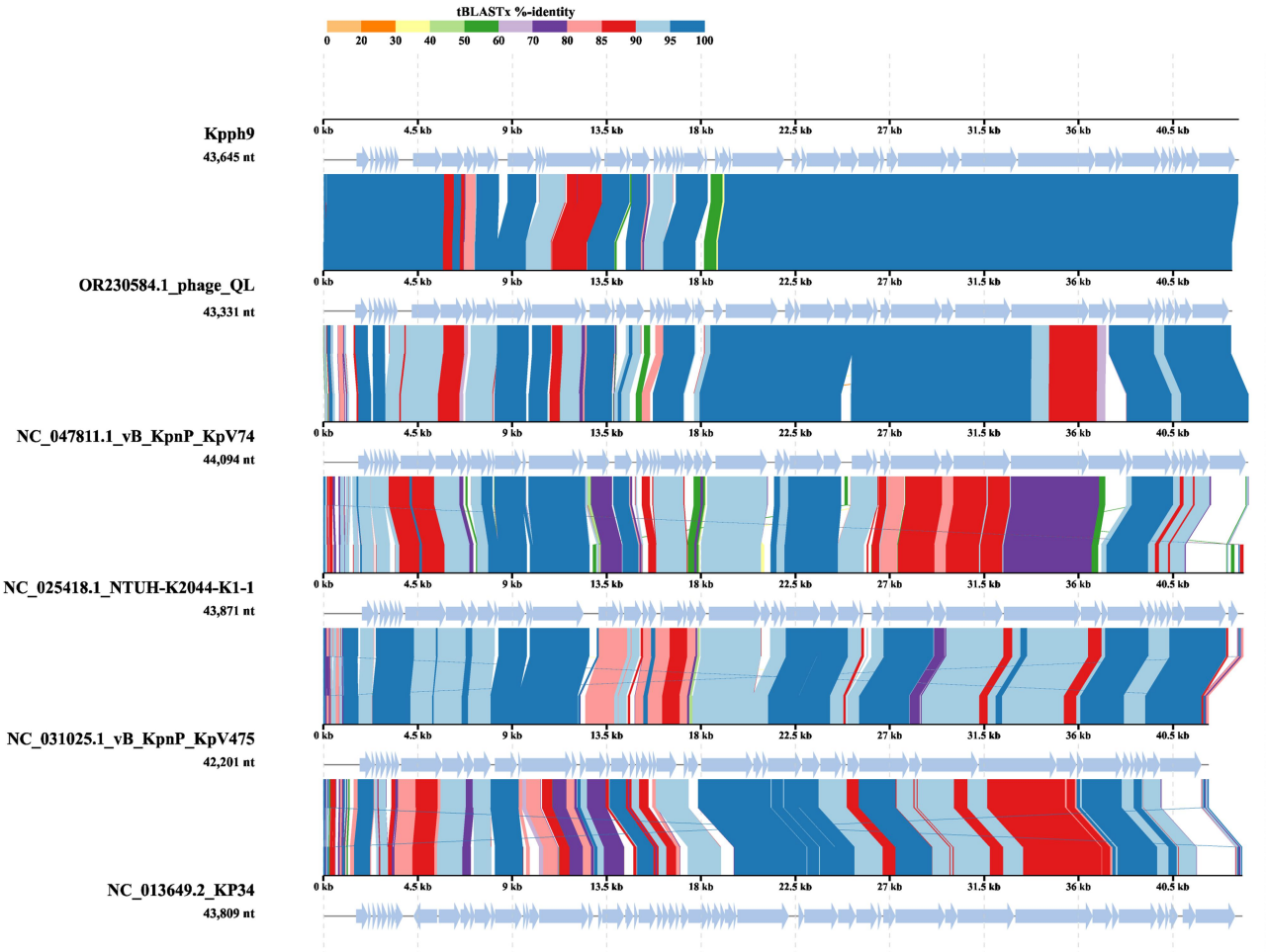

Figure 7. Genomic comparative analysis of Kpph9 and the mostly related phages in *Drulisvirus* genus was preformed using viptree based on genome-wide sequence similarities.

NUHL30457, both phages effectively reduced the viable host cell count and inhibited the host growth. They also suppressed host biofilm formation and notably disrupted mature biofilms. Both phages can tolerate a wide range of temperature and pH, exhibiting strong environmental tolerance and high storage stability. Genome analysis did not reveal integrase, antibiotic resistance, or virulence genes, indicating that both phages hold promise as components of a targeted "phage cocktail" against Hv-CRKp.

According to the *Klebsiella* phage data retrieved from the NCBI database (Supplementary Fig. S6), *Autographiviridae* and *Drexlerviridae* are two of the most abundant families of submitted *Klebsiella* phages, with 216 (38%) and 95 (17%) complete genomes, respectively (Supplementary Fig. S6). Previously reported K2 type-specific phages were predominantly found in the *Webervirus* genus of Drexlerviridae family and the *Drulisvirus* genus of Autographiviridae family, such as GH-K3, RAD2, KLPN1, and KpV74 [53–56]. In addition to K2 capsular type, phages from the *Webervirus* genus and *Drulisvirus* genus can target K1, K34, and K63 capsular type of *K. pneumoniae*, such as NTUH-K2044-K1-1, KpV71, KpV475, and Kp34. This indicates the extensive potential of these two phage families for clinical applications in treating infections caused by hypervirulent and drug-resistant *K. pneumoniae* [57]. To elucidate the evolutionary relationships among phages with varied host ranges within the same genus, multiple conserved single-copy protein sequences were selected and concatenated into a single alignment for both the *Webervirus* and *Drulisvirus* genera, separately. As expected, distinct marker genes were selected in these two genera, highlighting the absence of universally conserved markers due to their diverse genomic mosaicism [57]. Consequently, our findings suggest that individual conserved genes, such as the terminase and major capsid protein, may not be suitable for phylogenetic analyses and classifications at or above the family level [58]. Additionally, the careful selection of marker genes is crucial to minimize biases in phylogenetic

inference. Phylogenetic analyses have shown that phages with higher nucleotide similarities and analogous host ranges tend to cluster together, but exceptions may exist, as seen in cases like Kpph1 and KOX1. Genomic variations between these two phages are mainly observed in the depolymerase region, indicating distinct co-evolutionary pathways between the phages and their respective hosts.

In addition to obtaining drug-resistant genes, bacteria have the ability to develop multicellular structures called biofilms, which serve as a protective shield and render the cells impenetrable to antibiotics and immune clearance. The biofilm state offers superior adaptive advantages compared to the planktonic form, leading to its prevalence as the dominant phenotype in nearly all habitats on Earth. For instance, the National Institutes of Health (NIH) has revealed that over 80% of chronic bacterial infections in the body are attributed to biofilms [59]. Furthermore, biofilms can form on medical devices and implantable materials. Consequently, there is an urgent need to develop alternative therapeutic strategies to address bacterial biofilms. A biofilm is primarily an aggregate of microorganisms and EPS. Recent studies have revealed that phage-encoded enzymes can degrade the EPS within biofilm matrix, thereby enhancing phage diffusion and attachment [30]. In this study, phage Kpph1 and Kpph9 demonstrated efficacy in preventing the biofilm formation and disrupting the mature biofilm matrix, comparable to the previously reported *Klebsiella* phages vB_Kpn_ZCKp20p and PG14 [30,31]. These results suggest that both phages carry potential EPS depolymerases that effectively target Hv-CRKp biofilms. Interestingly, the MOI influenced the phages' ability to inhibit biofilm formation. Groups that had higher concentrations of phages demonstrated more effective inhibition of biofilm formation. However, when treating mature biofilms, phages at all MOIs exhibited consistent antibiofilm effects. These outcomes align with earlier studies and highlight the efficacy of phage-derived enzymes in combating biofilms, even at low concentrations [30].

The CPS of *K. pneumoniae* act as a protective shield, enabling the pathogen to resist antibiotics and evade the host's immune response. To penetrate the bacterial boundary, phages can encode depolymerases that specifically degrade the CPS of distinct capsular types. Recent studies have demonstrated that depolymerases not only facilitate the binding and degradation of the CPS, but also disrupt biofilms and reduce bacterial virulence, underscoring a significant role of depolymerases in phage infections and interactions with the host [60]. Phage adsorption stands as the initial stage of infection, serving as a critical factor in determining host specificity. Phages containing a single depolymerase that targets a specific capsular bacterial type indicate the potential use of capsular type-specific depolymerases for precise capsular typing [61]. Due to the high host specificity of these phages, the microbiome linked to the targeted pathogens could remain unaffected during phage infection. Therefore, phages and phage-encoded depolymerases offer promising alternative strategies for the identification and inactivation of specific pathobionts within the human microbiome. Studies investigating phage depolymerases against *K. pneumoniae* and their potential therapeutic effects have been reported. For instance, depolymerase K4–26 derived from phage K4–26 has been shown to reduce virulence and boost the sensitivity of *K. aerogenes* 4–26 to innate immunity [17]. Additionally, DepoKP36, produced by the *Klebsiella* phage KP36, significantly inhibited the growth of the K36-type *K. pneumoniae* in the *Galleria mellonella* larvae model [62]. Dep42, derived from the *Klebsiella* phage SH-KP152226, has demonstrated remarkable antibacterial and antibiofilm activities against *K. pneumoniae* capsular type K47 and could also augment the activity of polymyxin in degrading biofilms [63]. Two depolymerases, Dep_kpv79 and Dep_kpv767, have been observed to increase survival rates of mice infected with K57-type *K. pneumoniae* [64]. In the light of these findings and considering the pathogenicity and lethality of the K2 capsular type of *K. pneumoniae*, potential depolymerases from Kpph1 and Kpph9 phages were explored. In this study, both isolated phages were found to harbor two potential depolymerases targeting K2 type *K. pneumoniae*. ORF20 of Kpph1 was annotated as a depolymerase, and demonstrated high structural identity with the depolymerase of *Klebsiella* phage GH-K3 and RAD2. The depolymerases of GH-K3 and RAD2 have been characterized and their cryo-EM structures have been uncovered. Characterized depolymerases contain a core region including a short neck helix and a connection domain, a β-helix domain, a connection helix domain, a carbohydrate-binding domain, and a C-terminal domain. The identified K2-specific depolymerases have the ability to break down the K2-type CPS and promote the bounding of unencapsulated strains to complement C3, thus triggering complement-mediated opsonophagocytosis.

Interestingly, although Kpph1 exhibit high genomic similarity with phage KOX1, IMGroot, and Call, its depolymerase share greater similarity to sequences

found in RAD2 and GH-K3. A phylogenetic tree constructed from conserved protein sequences illustrated that the Kpph1 depolymerase forms a cluster with RAD2 and GH-K3, setting it apart from another cluster consisting of IMGroot, Call, and Kp36. Kp36, serving as the reference phage species of the *Webervirus* genus, encodes a depolymerase that efficiently targets the K63 type *K. pneumoniae* [65]. Despite sharing a 75.91% nucleotide similarity with Kp36, the depolymerases of Kpph1 and Kp36 only exhibit a 41.4% identity. Moreover, the predicted three-dimensional structures of each protein yielded different models, with Kp36 showing 41.94% sequence identity with 8bke.1.A (*Klebsiella* phage KP34p57 capsular depolymerase) and Kpph1 exhibiting 97.79% identity with 7lzj.1.A (Dpk2 tail spike depolymerase). These findings may suggest that phages can acquire depolymerase sequences through recombination events, and leading to divergence in host range among phage species within the same genus. Furthermore, ORF19 of Kpph1 has been identified as a central tail fiber protein harboring a domain predicted to be pectate lyase, a crucial domain implicated in *Klebsiella* phage depolymerases [66]. While, this region is highly conserved in the selected genomes of *Webervirus* genus, the precise function of this protein remains undefined. It could play a pivotal role in host interactions, including phage recognition, binding, and degradation of capsular polysaccharides. Although ORF48 and ORF56 of Kpph9 have been predicted to be tail fiber proteins, they share limited sequence and structural similarities with known phage proteins. Research has previously demonstrated that phages equipped with multiple depolymerases can target hosts with various capsular types, underscoring the importance of depolymerases in determining host specificity. The host-specificity of the two putative depolymerase sequences and their roles at different stages of phage infection remain uncertain. Consequently, further investigation is necessary to elucidate the roles of these putative tail fiber proteins in the host lysis process of Kpph1 and Kpph9.

Conclusion

This study involved the isolation of two virulent phages that target the K2-type Hv-CRKp strain of *K. pneumoniae*, followed by comprehensive biophysiological and bioinformatic analyses. These phages exhibited exceptional lytic efficacy against their carbapenem-resistant, hypervirulent host and demonstrated noteworthy stability under a broad range of temperatures and pH values. Genomic analysis revealed the absence of integrase, antibiotic resistance, or virulence genes, indicating that the phages are promising agents for managing and treating infections by Hv-CRKp *K. pneumoniae*. Furthermore, these phages could serve as potential sources of prospective antibacterial and antibiofilm enzymes identified in their genomes. Further characterizations are warranted to verify the functions of the postulated depolymerases and their mechanisms of antibacterial and antibiofilm activity.

Disclosure statement

No potential conflict of interest was reported by the author(s).

Funding

This work was supported by the National Natural Science Foundation of China [32300103 and 82360399], Natural Science Foundation of Jiangxi Province [20224BAB216081 and 20212BAB216041], Major Discipline Academic and Technical Leader Cultivation Project of Jiangxi Province [20243BCE51133], Partnership Grant From The Central Government Guides Local Funds For Scientific And Technological Development [20221ZDG020070], and Hospital Foundation of Talent Research and Cultivation [YFYPY202276].

Author contributions

Ye. H.: data curation, visualization, investigation, and writing-original draft preparation. **Yuan. H**: data analysis and validation. **Z.P. W.**: sample collection, processing, and phage isolation. **Z.Y. F.**: phage purification and characterization. **F.L. Z.**: writing-reviewing and editing. **Y. L**: strain supply and writing revision. **X.P. X.**: conceptualization, methodology, and supervision. All authors have read and approved the final version of the manuscript.

Data availability statement

The genome sequence data for phages Kpph1 and Kpph9 have been submitted to the GenBank database at the National Center for Biotechnology Information (NCBI) (https://www.ncbi.nlm.nih.gov/nuccore/) under accession numbers OR983331 and OR983332. The sequencing raw data and data used to generate the figures in this study have been uploaded to figshare (https://doi.org/10.6084/m9.figshare.25650717.v5).

ORCID

Ye Huang http://orcid.org/0000-0002-6952-3817
Xinping Xu http://orcid.org/0000-0002-9568-4171

References

[1] Dong N, Yang X, Chan E-C, et al. *Klebsiella* species: taxonomy, hypervirulence and multidrug resistance. EBioMedicine. 2022;79:103998. doi: 10.1016/j.ebiom.2022.103998

[2] WHO publishes list of bacteria for which new antibiotics are urgently needed [Internet]. https://www.who.int/news/item/27-02-2017-who-publishes-list-of-bacteria-for-which-new-antibiotics-are-urgently-needed

[3] Gu D, Dong N, Zheng Z, et al. A fatal outbreak of ST11 carbapenem-resistant hypervirulent *Klebsiella pneumoniae* in a Chinese hospital: a molecular epidemiological study. Lancet Infect Dis. 2018;18(1):37–46. doi: 10.1016/S1473-3099(17)30489-9

[4] Yang X, Dong N, Chan E-C, et al. Carbapenem resistance-encoding and virulence-encoding conjugative plasmids in *Klebsiella pneumoniae*. Trends Microbiol. 2021;29(1):65–83. doi: 10.1016/j.tim.2020.04.012

[5] Tian D, Liu X, Chen W, et al. Prevalence of hypervirulent and carbapenem-resistant *Klebsiella pneumoniae* under divergent evolutionary patterns. Emerg Microbes Infect. 2022;11(1):1936–1949. doi: 10.1080/22221751.2022.2103454

[6] Du H, Wang T, Chen L. Virulence factors in hypervirulent *Klebsiella pneumoniae*. Front Microbiol. 2021;12:642484. doi: 10.3389/fmicb.2021.642484

[7] Paczosa MK, Mecsas J. *Klebsiella pneumoniae*: going on the offense with a strong defense. Microbiol Mol Biol Rev. 2016;80(3):629–661. doi: 10.1128/MMBR.00078-15

[8] Opoku-Temeng C, Kobayashi SD, DeLeo FR. *Klebsiella pneumoniae* capsule polysaccharide as a target for therapeutics and vaccines. Comput Struct Biotechnol J. 2019;17:1360–1366. doi: 10.1016/j.csbj.2019.09.011

[9] Rendueles O. Deciphering the role of the capsule of *Klebsiella pneumoniae* during pathogenesis: a cautionary tale. Mol Microbiol. 2020;113(5):883–888. doi: 10.1111/mmi.14474

[10] Follador R, Heinz E, Wyres KL, et al. The diversity of *Klebsiella pneumoniae* surface polysaccharides. Microb Genomics. 2016;2(8):e00073. doi: 10.1099/mgen.0.000073

[11] Lin Y-T, Siu LK, Lin J-C, et al. Seroepidemiology of *Klebsiella pneumoniae* colonizing the intestinal tract of healthy Chinese and overseas Chinese adults in Asian countries. BMC Microbiol. 2012;12(1):13. doi: 10.1186/1471-2180-12-13

[12] Choby JE, Howard-Anderson J, Weiss DS. Hypervirulent *Klebsiella pneumoniae* – clinical and molecular perspectives. J Intern Med. 2020;287(3):283–300. doi: 10.1111/joim.13007

[13] Guo Z, Liu M, Zhang D. Potential of phage depolymerase for the treatment of bacterial biofilms. Virulence. 2023;14(1):2273567. doi: 10.1080/21505594.2023.2273567

[14] MacNair CR, Rutherford ST, Tan M-W. Alternative therapeutic strategies to treat antibiotic-resistant pathogens. Nat Rev Microbiol. 2024;22(5):262–275. doi: 10.1038/s41579-023-00993-0

[15] Wang H, Liu Y, Bai C, et al. Translating bacteriophage-derived depolymerases into antibacterial therapeutics: challenges and prospects. Acta Pharm Sin B. 2024;14(1):155–169. doi: 10.1016/j.apsb.2023.08.017

[16] Knecht LE, Veljkovic M, Fieseler L. Diversity and function of phage encoded depolymerases. Front Microbiol. 2020;10:2949. doi: 10.3389/fmicb.2019.02949

[17] Cui X, Du B, Feng J, et al. A novel phage carrying capsule depolymerase effectively relieves pneumonia caused by multidrug-resistant *Klebsiella aerogenes*. J Biomed Sci. 2023;30(1):75. doi: 10.1186/s12929-023-00946-y

[18] Pertics BZ, Cox A, Nyúl A, et al. Isolation and characterization of a novel lytic bacteriophage against the K2 capsule-expressing hypervirulent *Klebsiella pneumoniae* strain 52145, and identification of its functional depolymerase. Microorganisms. 2021;9(3):650. doi: 10.3390/microorganisms9030650

[19] Cai R, Ren Z, Zhao R, et al. Structural biology and functional features of phage-derived depolymerase Depo32 on *Klebsiella pneumoniae* with K2 serotype capsular polysaccharides. Microbiol Spectr. 2023;11(5):e05304–22. doi: 10.1128/spectrum.05304-22

[20] Ye T-J, Fung K-M, Lee I-M, et al. *Klebsiella pneumoniae* K2 capsular polysaccharide degradation by a bacteriophage depolymerase does not require trimer formation. MBio. 2024;15(3):e03519–23. doi: 10.1128/mbio.03519-23

[21] Liu Y, Long D, Xiang T-X, et al. Whole genome assembly and functional portrait of hypervirulent extensively drug-resistant NDM-1 and KPC-2 co-producing *Klebsiella pneumoniae* of capsular serotype K2 and ST86. J Antimicrob Chemother. 2019;74(5):1233–1240. doi: 10.1093/jac/dkz023

[22] Luong T, Salabarria A-C, Edwards RA, et al. Standardized bacteriophage purification for personalized phage therapy. Nat Protoc. 2020;15(9):2867–2890. doi: 10.1038/s41596-020-0346-0

[23] Bonilla N, Barr JJ. Phage on tap: a quick and efficient protocol for the preparation of bacteriophage laboratory stocks. Methods Mol Biol. 2018;1838:37–46.

[24] Uskudar-Guclu A, Unlu S, Salih-Dogan H, et al. Biological and genomic characteristics of three novel bacteriophages and a phage-plasmid of *Klebsiella pneumoniae*. Can J Microbiol. 2024;70(6):213–225. doi: 10.1139/cjm-2023-0188

[25] Liu B, Zheng T, Quan R, et al. Biological characteristics and genomic analysis of a novel *Vibrio parahaemolyticus* phage phiTY18 isolated from the coastal water of Xiamen China. Front Cell Infect Microbiol. 2022;12:1035364. doi: 10.3389/fcimb.2022.1035364

[26] Kropinski AM. Practical advice on the one-step growth curve. Methods Mol Biol. 2018;1681:41–47.

[27] Hyman P, Abedon ST. Practical methods for determining phage growth parameters. Methods Mol Biol. 2009;501:175–202.

[28] Bai J, Zhang F, Liang S, et al. Isolation and characterization of vB_kpnm_17–11, a novel phage efficient against carbapenem-resistant *Klebsiella pneumoniae*. Front Cell Infect Microbiol. 2022;12:897531. doi: 10.3389/fcimb.2022.897531

[29] Blundell-Hunter G, Enright MC, Negus D, et al. Characterisation of bacteriophage-encoded depolymerases selective for key *Klebsiella pneumoniae*

capsular exopolysaccharides. Front Cell Infect Microbiol. 2021;11:686090. doi: 10.3389/fcimb.2021.686090

[30] Zaki BM, Fahmy NA, Aziz RK, et al. Characterization and comprehensive genome analysis of novel bacteriophage, vB_kpn_zckp20p, with lytic and anti-biofilm potential against clinical multidrug-resistant *Klebsiella pneumoniae*. Front Cell Infect Microbiol. 2023;13:1077995. doi: 10.3389/fcimb.2023.1077995

[31] Sambrook J, Russell DW. Purification of nucleic acids by extraction with phenol: chloroform. CSH Protocol. 2006;2006(1):db.prot4455. doi: 10.1101/pdb.prot4455

[32] Chen Y, Chen Y, Shi C, et al. Soapnuke: a MapReduce acceleration-supported software for integrated quality control and preprocessing of high-throughput sequencing data. Gigascience. 2018;7(1):gix120. doi: 10.1093/gigascience/gix120

[33] Li H, Durbin R. Fast and accurate short read alignment with Burrows–Wheeler transform. Bioinformatics. 2009;25(14):1754–1760. doi: 10.1093/bioinformatics/btp324

[34] Li D, Liu C-M, Luo R, et al. MEGAHIT: an ultra-fast single-node solution for large and complex metagenomics assembly via succinct *de Bruijn* graph. Bioinformatics. 2015;31(10):1674–1676. doi: 10.1093/bioinformatics/btv033

[35] Nayfach S, Camargo AP, Schulz F, et al. CheckV assesses the quality and completeness of metagenome-assembled viral genomes. Nat Biotechnol. 2021;39(5):578–585. doi: 10.1038/s41587-020-00774-7

[36] Danecek P, Bonfield JK, Liddle J, et al. Twelve years of SAMtools and BCFtools. Gigascience. 2021;10(2):giab008. doi: 10.1093/gigascience/giab008

[37] Tynecki P, Guziński A, Kazimierczak J, et al. PhageAI - bacteriophage life cycle recognition with machine learning and natural language processing. Bioinformatics. 2020. Available from: http://biorxiv.org/lookup/doi/10.1101/2020.07.11.198606

[38] Aziz RK, Bartels D, Best AA, et al. The RAST server: rapid annotations using subsystems technology. BMC Genomics. 2008;9(1):75. doi: 10.1186/1471-2164-9-75

[39] McNair K, Zhou C, Dinsdale EA, et al. PHANOTATE: a novel approach to gene identification in phage genomes. Bioinformatics. 2019;35(22):4537–4542. doi: 10.1093/bioinformatics/btz265

[40] Chan PP, Lin BY, Mak AJ, et al. tRnascan-se 2.0: improved detection and functional classification of transfer RNA genes. Nucleic Acids Res. 2021;49(16):9077–9096. doi: 10.1093/nar/gkab688

[41] Liu B, Zheng D, Zhou S, et al. VFDB 2022: a general classification scheme for bacterial virulence factors. Nucleic Acids Res. 2022;50(D1):D912–D917. doi: 10.1093/nar/gkab1107

[42] Florensa AF, Kaas RS, Clausen PTLC, et al. ResFinder – an open online resource for identification of antimicrobial resistance genes in next-generation sequencing data and prediction of phenotypes from genotypes. Microb Genomics. 2022;8(1):000748. doi: 10.1099/mgen.0.000748

[43] Grant JR, Enns E, Marinier E, et al. Proksee: in-depth characterization and visualization of bacterial genomes. Nucleic Acids Res. 2023;51(W1):W484–W492. doi: 10.1093/nar/gkad326

[44] Cantu VA, Salamon P, Seguritan V, et al. PhANNs, a fast and accurate tool and web server to classify phage structural proteins. PLOS Comput Biol. 2020;16(11):e1007845. doi: 10.1371/journal.pcbi.1007845

[45] Zimmermann L, Stephens A, Nam S-Z, et al. A completely reimplemented mpi bioinformatics toolkit with a new HHpred server at its core. J Mol Biol. 2018;430(15):2237–2243. doi: 10.1016/j.jmb.2017.12.007

[46] Waterhouse A, Bertoni M, Bienert S, et al. SWISS-MODEL: homology modelling of protein structures and complexes. Nucleic Acids Res. 2018;46(W1):W296–W303. doi: 10.1093/nar/gky427

[47] Page AJ, Cummins CA, Hunt M, et al. Roary: rapid large-scale prokaryote pan genome analysis. Bioinformatics. 2015;31(22):3691–3693. doi: 10.1093/bioinformatics/btv421

[48] Katoh K, Standley DM. MAFFT multiple sequence alignment software version 7: improvements in performance and usability. Mol Biol Evol. 2013;30(4):772–780. doi: 10.1093/molbev/mst010

[49] Kumar S, Stecher G, Tamura K. MEGA7: molecular evolutionary genetics analysis version 7.0 for bigger datasets. Mol Biol Evol. 2016;33(7):1870–1874. doi: 10.1093/molbev/msw054

[50] Moraru C, Varsani A, Kropinski AM. Viridic—a novel tool to calculate the intergenomic similarities of prokaryote-infecting viruses. Viruses. 2020;12(11):1268. doi: 10.3390/v12111268

[51] Nishimura Y, Yoshida T, Kuronishi M, et al. ViPTree: the viral proteomic tree server. Bioinformatics. 2017;33(15):2379–2380. doi: 10.1093/bioinformatics/btx157

[52] Grigson SR, Giles SK, Edwards RA, et al. Knowing and naming: phage annotation and nomenclature for phage therapy. Clin Infect Dis. 2023;77(Supplement_5):S352–S359. doi: 10.1093/cid/ciad539

[53] Hoyles L, Murphy J, Neve H, et al. *Klebsiella pneumoniae* subsp. *pneumoniae* –bacteriophage combination from the caecal effluent of a healthy woman. PeerJ. 2015;3:e1061. doi: 10.7717/peerj.1061

[54] Cai R, Wang Z, Wang G, et al. Biological properties and genomics analysis of vB_kpns_GH-K3, a *Klebsiella* phage with a putative depolymerase-like protein. Virus Genes. 2019;55(5):696–706. doi: 10.1007/s11262-019-01681-z

[55] Dunstan RA, Bamert RS, Belousoff MJ, et al. Mechanistic insights into the capsule-targeting depolymerase from a *Klebsiella pneumoniae* bacteriophage. Goldberg JB, editor. Microbiol Spectr. 2021;9(1):e01023–21. doi: 10.1128/Spectrum.01023-21

[56] Volozhantsev NV, Borzilov AI, Shpirt AM, et al. Comparison of the therapeutic potential of bacteriophage KpV74 and phage-derived depolymerase (β-glucosidase) against *Klebsiella pneumoniae* capsular type K2. Virus Res. 2022;322:198951. doi: 10.1016/j.virusres.2022.198951

[57] Drulis-Kawa Z, Mackiewicz P, Kęsik-Szeloch A, et al. Isolation and characterisation of KP34—a novel φKMV-like bacteriophage for *Klebsiella pneumoniae*. Appl Microbiol Biotechnol. 2011;90(4):1333–1345. doi: 10.1007/s00253-011-3149-y

[58] Low SJ, Džunková M, Chaumeil P-A, et al. Evaluation of a concatenated protein phylogeny for classification of tailed

double-stranded DNA viruses belonging to the order *Caudovirales*. Nat Microbiol. 2019;4(8):1306–1315. doi: 10.1038/s41564-019-0448-z

[59] Rumbaugh KP, Sauer K. Biofilm dispersion. Nat Rev Microbiol. 2020;18(10):571–586. doi: 10.1038/s41579-020-0385-0

[60] Dunstan RA, Bamert RS, Tan KS, et al. Epitopes in the capsular polysaccharide and the porin OmpK36 receptors are required for bacteriophage infection of *Klebsiella pneumoniae*. Cell Rep. 2023;42(6):112551. doi: 10.1016/j.celrep.2023.112551

[61] Hsu C-R, Lin T-L, Pan Y-J, et al. Isolation of a bacteriophage specific for a new capsular type of *Klebsiella pneumoniae* and characterization of its polysaccharide depolymerase. PLOS ONE. 2013;8(8): e70092. doi: 10.1371/journal.pone.0070092

[62] Majkowska-Skrobek G, Łątka A, Berisio R, et al. Capsule-targeting depolymerase, derived from *Klebsiella* KP36 phage, as a tool for the development of anti-virulent strategy. Viruses. 2016;8(12):324. doi: 10.3390/v8120324

[63] Wu Y, Wang R, Xu M, et al. A novel polysaccharide depolymerase encoded by the phage sh-kp152226 confers specific activity against multidrug-resistant *Klebsiella pneumoniae* via biofilm degradation. Front Microbiol. 2019;10:2768. doi: 10.3389/fmicb.2019.02768

[64] Volozhantsev N V, Shpirt A M, Borzilov A I, et al. Characterization and therapeutic potential of bacteriophage-encoded polysaccharide depolymerases with β galactosidase activity against *Klebsiella pneumoniae* K57 capsular type. Antibiotics. 2020;9(11):732. doi: 10.3390/antibiotics9110732

[65] Kęsik-Szeloch A, Drulis-Kawa Z, Weber-Dąbrowska B, et al. Characterising the biology of novel lytic bacteriophages infecting multidrug resistant *Klebsiella pneumoniae*. Virol J. 2013;10(1):100. doi: 10.1186/1743-422X-10-100

[66] Pires DP, Oliveira H, Melo LDR, et al. Bacteriophage-encoded depolymerases: their diversity and biotechnological applications. Appl Microbiol Biotechnol. 2016;100 (5):2141–2151. doi: 10.1007/s00253-015-7247-0